

## Evaluating AURA/OMI ozone profiles using ozonesonde data and EPA surface measurements for August 2006

Lihua Wang<sup>a</sup>, M.J. Newchurch<sup>a,\*</sup>, Arastoo Biazar<sup>b</sup>, Xiong Liu<sup>c</sup>, Shi Kuang<sup>a</sup>, Maudood Khan<sup>d</sup>, Kelly Chance<sup>c</sup>

<sup>a</sup> Atmospheric Science Department, University of Alabama in Huntsville, Huntsville, AL 35805, USA

<sup>b</sup> National Space Science & Technology Center, University of Alabama in Huntsville, Huntsville, AL 35805, USA

<sup>c</sup> Atomic and Molecular Physics Division, Harvard-Smithsonian Center for Astrophysics, Cambridge, MA 02138, USA

<sup>d</sup> The Universities Space Research Association, USA

### ARTICLE INFO

#### Article history:

Received 3 November 2010

Received in revised form

1 June 2011

Accepted 3 June 2011

#### Keywords:

OMI

IONS06

CMAQ

EPA

Ozone evaluation

### ABSTRACT

We evaluate the Ozone Monitoring Instrument (OMI) ozone profile retrieval against ozonesonde data and the Environmental Protection Agency (EPA) surface measurements for August 2006. Comparison of individual OMI ozone profile with ozonesonde indicates that OMI ozone profile can explain the general vertical variation of ozone but is limited in observing the boundary layer ozone, due to weak sensitivity to boundary layer ozone and thick lowest layer (~2.5 km). We made pair-wise comparison between OMI and ozonesondes on 24 OMI vertical layers, as well as the 39 sigma-P vertical layers of the Community Multi-scale Air Quality (CMAQ) modeling system, respectively. OMI shows reasonable agreement with ozonesonde in the lower- to mid-troposphere. In the upper troposphere, while the bias increases, the normalized bias does not show much variation and remains below 10%. Comparison with EPA's surface-monitoring data indicates that OMI observations at the lowest layer (surface to 2.5 km altitude) represent the mean values. While OMI underestimates elevated ozone concentrations, it explains the larger-scale spatial variation seen in the surface monitors.

© 2011 Elsevier Ltd. All rights reserved.

### 1. Introduction

Satellite retrievals of trace gases at high spatial resolution and with daily global coverage, have significant potential in improving air-pollution model simulation, in the areas of data assimilation and model evaluation. In a recent research project, we tried to improve chemical model accuracy by applying a direct satellite retrieval of tropospheric ozone profiles as boundary conditions and initial conditions. For this to be useful, we need to evaluate the accuracy of these satellite-retrieved O<sub>3</sub> profiles, both in the free troposphere and near the surface.

The Ozone Monitoring Instrument (OMI), launched in July 2004 on the EOS Aura satellite, measures nadir-viewing backscattered radiances in the ultraviolet (UV) and visible (270–500 nm) (Levelt et al., 2006) with a daily global coverage. A newly-available off-line product of ozone profiles including tropospheric ozone is retrieved from UV radiances in the spectral region 270–330 nm using the optimal estimation technique (Liu et al., 2005, 2007, 2010). Ozone

profiles are retrieved at 24 layers (~2.5 km thick per layer) from surface to about 60 km. The spatial resolution is 13 km-by-48 km at nadir; the vertical resolution ranges from ~7–11 km in the stratosphere to ~10–14 km in the troposphere. The retrieved profiles are capable of capturing ozone perturbations caused by convection, biomass burning and anthropogenic pollution in the troposphere (Liu et al., 2010). Validation against long-term ozonesonde data for 2004–2008 shows that, on average, OMI retrievals in the troposphere agree with ozonesonde observations to within 10% at middle latitudes (30N–60N) and the standard deviations are within 25%.

The INTEX Ozonesonde Network Study 2006 (IONS06) campaign launched 424 ozonesondes from 23 North American sites during August 2006, and thus provides an excellent dataset to evaluate OMI ozone profile retrievals (Thompson et al., 2008). In this study we take advantage of ozonesonde profiles measured at 18 ozonesonde stations (Fig. 1) during the IONS06 campaign.

In addition to the IONS06 data, EPA-monitored surface-ozone concentrations (hourly) at 1188 stations over the continental U.S. allow the evaluation of the accuracy and usefulness of OMI ozone profiles at the surface.

\* Corresponding author. Tel.: +1 2569617825; fax: +1 2569617755.

E-mail address: [mike@nsstc.uah.edu](mailto:mike@nsstc.uah.edu) (M.J. Newchurch).

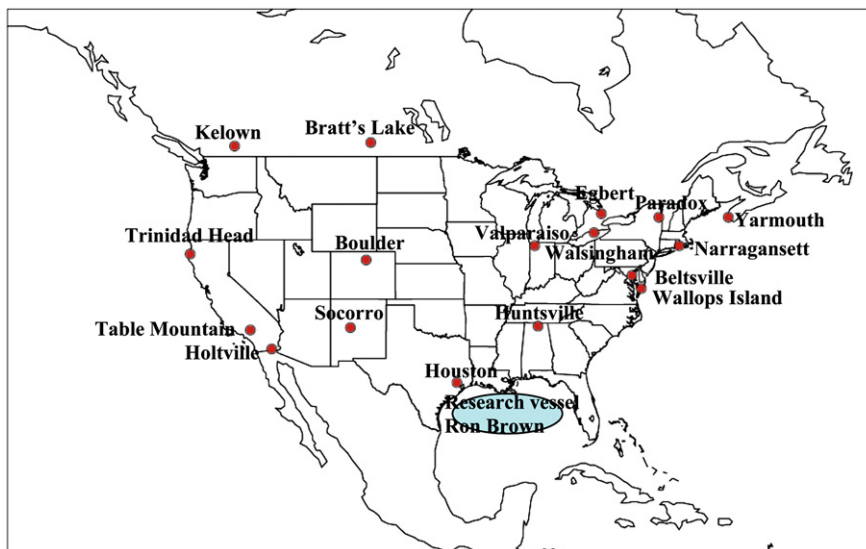


Fig. 1. 18 IONS06 operational sites that provide ozonesonde measurements for OMI ozone profile evaluation.

## 2. Direct comparison of individual OMI O<sub>3</sub> profiles with ozonesondes and TES observation

First, we made some direct comparisons between OMI ozone profiles and ozonesonde measurements at several sites. Fig. 2 presents an example of such a comparison. The figure shows ozonesonde measurements for the Ron Brown vessel on August 21 and August 30, 2006, alongside the closest OMI observations. The OMI observations are about 1–2 h behind the ozonesonde observations. The distance from OMI footprint to sonde location is about 20–27 km on both days. Fig. 2 also shows two ozone profiles retrieved from the Tropospheric Emission Spectrometer (TES) observations, which have a finer vertical resolution (about 6–10 km) than the OMI profiles whose vertical resolution in the

troposphere is about 10–14 km. The TES footprint is 224 km and 61 km away from the sonde locations on August 21 and August 30, respectively. As shown in Fig. 2, both TES and OMI can explain the general vertical variation of ozone. Ozonesonde measurements indicate some fine-scale vertical structure and inhomogeneity. Satellite observations, however, are not able to capture these fine-scale variations because of their much coarser vertical resolution. The red curve in Figure B is the convolved ozonesonde profiles, to which we apply the TES-averaging kernel and constraint to account for the TES-measurement sensitivity and vertical resolution. We performed the convolution according to the following equation (Rodgers, 2000; Rodgers and Connor, 2003; Worden et al., 2007):

$$\hat{\chi} = x_a + A(x - x_a) + \epsilon \quad (1)$$

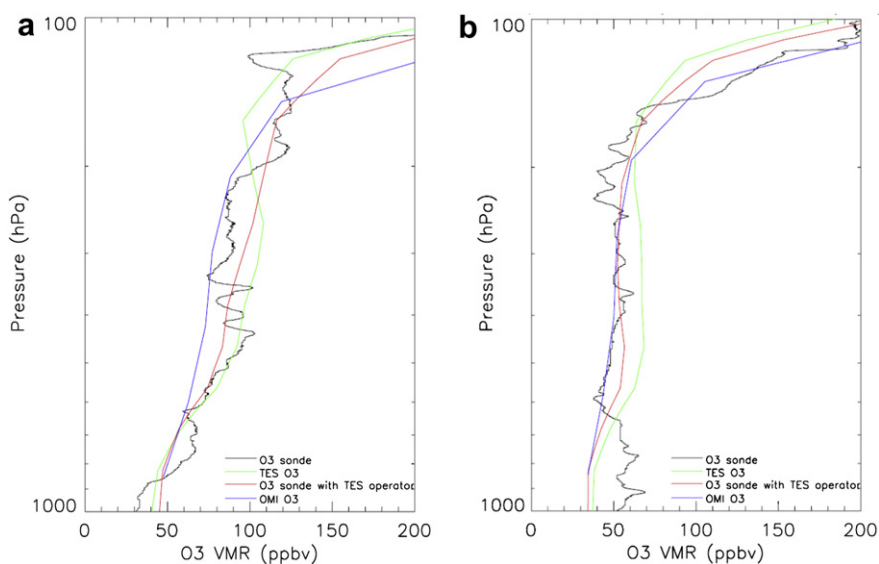


Fig. 2. An example of OMI, TES, ozonesonde comparison. a) Measurements for 8/21/2006, Ron Brown ozonesonde launched at (94.7W, 29.4N), 18:50 GMT, OMI O<sub>3</sub> measured at (94.8W, 29.2N), 19:54 GMT, distance from sonde = 20 km, TES O<sub>3</sub> measured at (97.0W, 29.2N), 19:53 GMT, distance from sonde = 224 km; b) Measurements for 8/30/2006, Ron Brown ozonesonde launched at (94.8W, 28.5N), 17:58 GMT, OMI O<sub>3</sub> measured at (94.7W, 28.7N), 19:47 GMT, distance from sonde = 28 km, TES O<sub>3</sub> measured at (95.2W, 28.2N), 19:47 GMT, distance from sonde = 61 km. The red lines in the figures are ozonesonde-convolved with TES-averaging kernel, which is a reconstruction of an ozonesonde profile for TES vertical resolution. (For interpretation of the references to colour in this figure legend, the reader is referred to the web version of this article.)

where  $x$  is the true state of the atmosphere,  $\hat{x}$  is the retrieved state,  $A$  is the averaging kernel, defined as the sensitivity of the retrieval  $\hat{x}$  to the true state  $x$ ,  $x_a$  is the a priori profile used in satellite retrievals, and  $\varepsilon$  is the measurement error (set to zero here). Assuming that the ozonesonde profile represents the true state of the atmospheric ozone ( $x$ ), and TES measures the same atmosphere simultaneously,  $\hat{x}$  gives TES-retrieved ozone profiles of this atmosphere. We refer to this retrieval as “convolved sonde profile” (red curves in Fig. 2), which is actually a reconstruction of the ozonesonde profile with TES vertical resolution and TES measurement sensitivity.

Fig. 2 also shows the limitation of OMI in observing the boundary layer ozone. OMI observation for the lowest layer usually represents the average concentration for a thick layer extending from surface to a height of approximately 2.5 km. This limitation is also seen when we compare OMI bottom-layer observations with EPA surface-monitoring ozone data.

### 3. Pair-wise comparison of OMI O<sub>3</sub> profiles with ozonesondes

#### 3.1. Comparison on OMI vertical resolution

We constructed 267 coincidence pairs between OMI and ozonesondes within the Continental U.S. during August 2006. The criteria for coincidence are that the OMI observation is close enough (<100 km distance) to the corresponding sonde station, and the sonde measurements are made within  $\pm 3$ -h range of the OMI observations. We convolve the ozonesonde profiles with OMI retrieval averaging kernels and a priori. Assuming that the ozonesonde measures the true state of atmospheric ozone concentration, the convolved ozonesonde represents what OMI retrieval will look like if OMI measures the atmosphere with the same resolution and sensitivity as the sonde does.

#### 3.2. OMI versus ozonesonde on model domain

Since our final goal of evaluating OMI ozone profiles is to apply OMI ozone data into chemistry-transport modeling (i.e., the Community Multi-scale Air Quality (CMAQ) modeling system), it's necessary to evaluate OMI data after mapping over the specific model resolution. We mapped both OMI ozone profiles and ozonesondes into 4-D CMAQ model domain and construct 244 coincidence pairs throughout the continental U.S. (CONUS) during the IONS-06 period. In each pair, OMI and sonde measure the same model grid cell. Most OMI measurements (at nadir) over the continental U.S. are made within 17:30 GMT (eastern area) and 20:30 GMT (western area). We use ozonesonde profiles measured during 15:00–23:00 GMT to construct the sonde-OMI coincidence pairs.

##### 3.2.1. Mapping OMI data onto CMAQ domain

Usually, 3–4 Aura orbits overpass the CONUS within a day, spanning over several hours. OMI has a very wide field-of-view ( $114^\circ$ ) with a cross-track swath width of 2600 km. The swath is binned to 30 positions across the track for the UV1 channel, at which resolution OMI ozone profiles are retrieved. The top-left and bottom-left panels in Fig. 3 show all of these OMI ozone observations combined, resulting in complete spatial coverage over the CONUS during August 21, 2006.

OMI pixel sizes (for used ozone profiles) approximately vary from 13 km (along-track)-by-48 km (across-track) to 24 km (along-track)-by-300 km (across-track). Different from OMI pixels, the CMAQ model has a 36 km-by-36 km equal-area grid setting. We design a “drop-in-box” method to re-sample OMI O<sub>3</sub> measurements onto the 36-km equal area CMAQ grid. For each OMI pixel that registered observations, we look for CMAQ grids whose centers fall within this OMI pixel and assign its O<sub>3</sub> profile retrieval to these CMAQ grids. Since some CMAQ grids at higher latitudes may

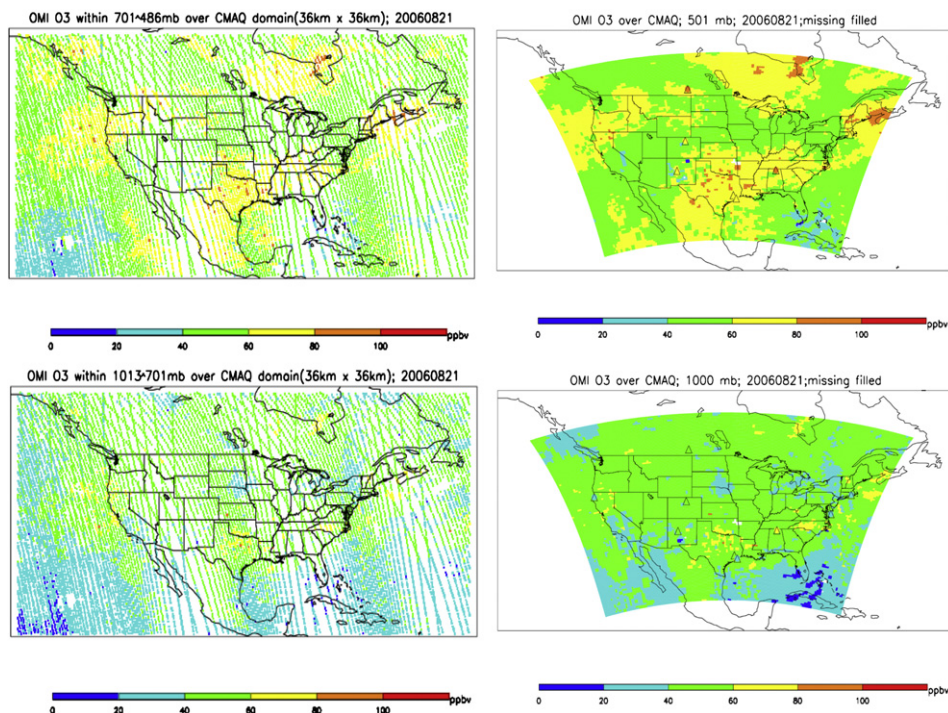


**Fig. 3.** Left: Aura/OMI Level 2 O<sub>3</sub> between 701–486 mb (top) and surface to 701 mb (bottom), plotted with fixed pixel size (not real size) to avoid overlap of neighboring pixels; Right: OMI O<sub>3</sub> mapped to CMAQ 3-D domain (36 km × 36 km, 39 layers), 501 mb (top) and 1000 mb (bottom). Ozonesondes from IONS06 are plotted as colored triangles. (For interpretation of the references to colour in this figure legend, the reader is referred to the web version of this article.)

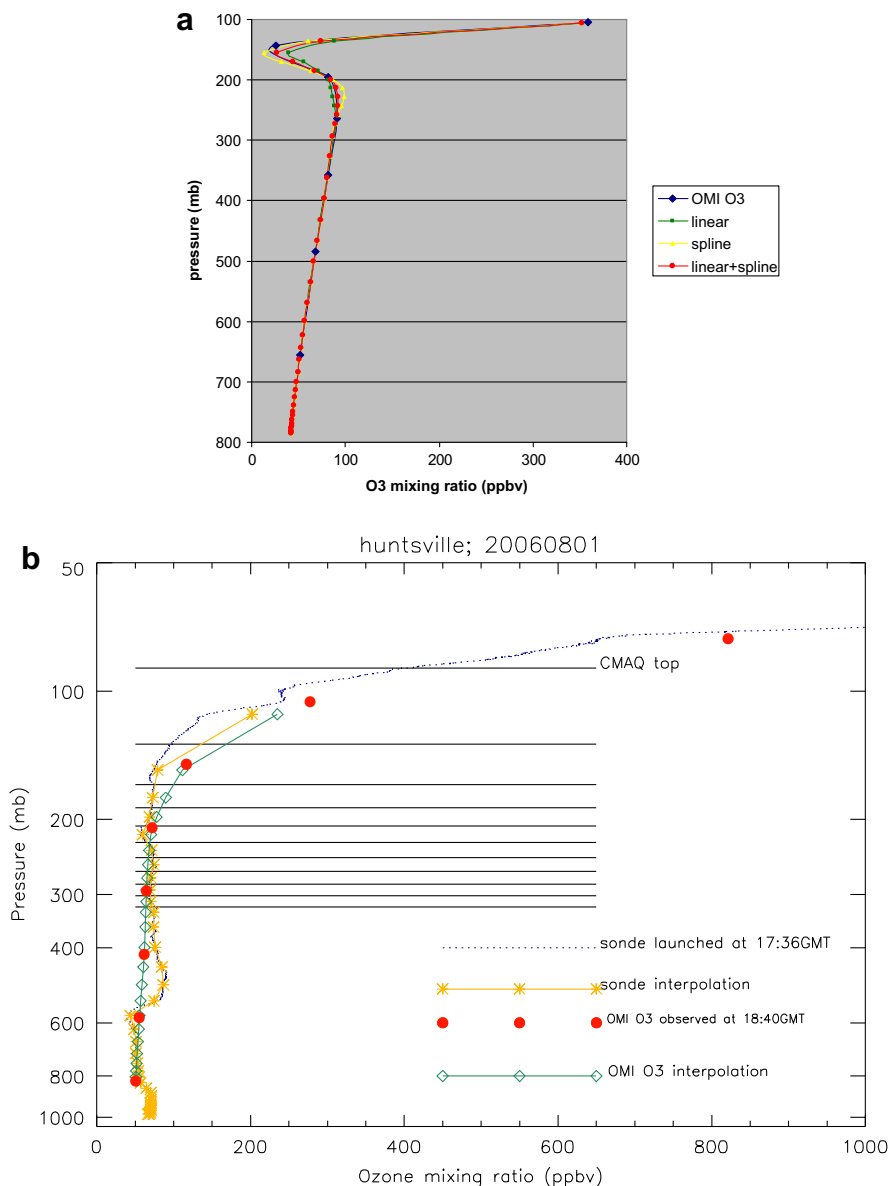


**Fig. 4.** (a) OMI O<sub>3</sub> observed at Boulder, CO on August 19, 2006 is interpolated onto CMAQ's 39 vertical layers using three different methods: linear, spline, and 50% linear plus 50% spline. (b) An example of re-sampling ozonesonde and OMI ozone profiles onto CMAQ's 39 vertical layers at Huntsville, AL on August 1, 2006. Re-sampled values are plotted at the middle of each CMAQ layer. Also shown are CMAQ vertical levels 30–40 with level 40 at CMAQ top.

receive more than one OMI O<sub>3</sub> value during a one-day period (due to overlap of OMI pixels measured during adjacent satellite orbits), we simply average these OMI O<sub>3</sub> profiles to get a mean value. Fig. 3 gives an example of mapping OMI O<sub>3</sub> to the CMAQ domain. The re-sampled OMI O<sub>3</sub> (top-right and bottom-right panels) shows the same spatial distribution patterns as the original OMI data does. We have filtered some OMI retrievals that do not converge or have large fitting residuals.

### 3.2.2. Vertical interpolation of OMI O<sub>3</sub> and ozonesonde onto CMAQ layers

On the vertical, CMAQ extends from surface up to 50 mb (hydrostatic) with 40  $\sigma$  levels ( $\sigma = 1$  at the surface and  $\sigma = 0$  at top; 39 layers):

$$\sigma = \frac{(P_{\text{hydro}} - P_{\text{top}})}{(P_{\text{sfc}} - P_{\text{top}})} \quad (2)$$

where  $P_{\text{hydro}}$ ,  $P_{\text{top}}$ ,  $P_{\text{sfc}}$  are hydrostatic pressures at the desired altitude, at the top of CMAQ atmosphere (fixed at 50 mb) and at the surface, respectively. We calculate the hydrostatic pressures ( $P_{\text{hydro}}$ ) for the middle of each  $\sigma$  layer and add the synoptic or local-scale pressure perturbations ( $P'$ ) to obtain the non-hydrostatic (dynamic) pressures  $P$ :

$$P = P_{\text{hydro}} + P' \quad (3)$$

Both OMI ozone profiles and ozonesonde data were mapped onto these non-hydrostatic pressure levels, representing the mean-mixing ratio within each  $\sigma$  layer. We choose CMAQ pressures at 19:00 GMT to perform the interpolation, considering that most OMI measurements (at nadir) over the continental U.S. are made within 17:30 GMT (eastern area) and 20:30 GMT (western area).

OMI originally retrieves O<sub>3</sub> as partial-column ozone (in units of DU) within each OMI vertical layers (~2.5-km thick each, totaling 24 layers from surface to ~60 km). We convert these partial-

column ozone values to layer-mean ozone-mixing ratio (ppbv) using the following formula (accurate to better than 1%) (Ziemke et al., 2001):

$$O_{3,i}(\text{ppbv}) = 1.251 \times O_{3,i}(\text{DU})/P_{i+1} - P_i \times (R/(R + Z_{\text{mid},i}))^2 \quad (4)$$

Where  $P_{i+1}$ ,  $P_i$  are the pressure in atm at two levels bounding layer  $i$ ;  $R$  is the radius of earth; and  $Z_{\text{mid},i}$  is the average altitude of that layer.

Usually linear interpolation gives similar results as spline interpolation does when interpolating OMI  $O_3$  (ppbv) onto CMAQ layers. However, when there are big changes in vertical ozone gradient, our test finds that a combination of linear interpolation and spline interpolation (50% linear plus 50% spline) gives the best fitting (Fig. 4(a)). Basically we expect to preserve the curvature of spline interpolation and use linear interpolation to reduce over-/under-shoots.

For ozonesonde profiles, we re-sample them onto CMAQ vertical layers by averaging all available sonde measurements within each CMAQ layer. Fig. 4(b) shows an example of re-sampling ozonesonde and OMI  $O_3$  profiles onto CMAQ vertical layers at Huntsville, AL on August 1, 2006.

Cases of mismatching surface pressures between OMI retrieval and CMAQ system are unavoidable. For example, one specific OMI profile estimates the surface pressure as 800 mb, while CMAQ indicates a surface pressure of 1000 mb. This kind of mismatch maybe either caused by the general inability of the OMI instrument to resolve the boundary-layer ozone for typical atmospheric conditions, or due to incorrect pressure simulation in the Pennsylvania State University/National Center for Atmospheric Research

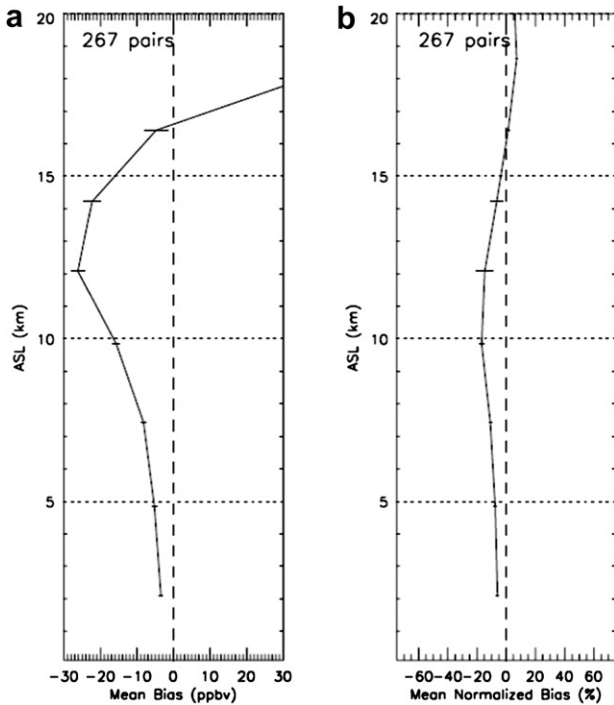


**Fig. 5.** OMI/ozonesonde comparison on OMI vertical resolution. Mean bias  $\left(\frac{1}{N} \sum_{i=1}^N (O_{3i}^{\text{OMI}} - O_{3i}^{\text{ozonesonde}})\right)$  and mean-normalized bias  $\left(\frac{1}{N} \sum_{i=1}^N \frac{(O_{3i}^{\text{OMI}} - O_{3i}^{\text{ozonesonde}})}{O_{3i}^{\text{ozonesonde}}}\right)$  from 267 pair of observations are presented, as well as the standard errors. Ozonesondes are convolved with OMI averaging kernels and a priori.

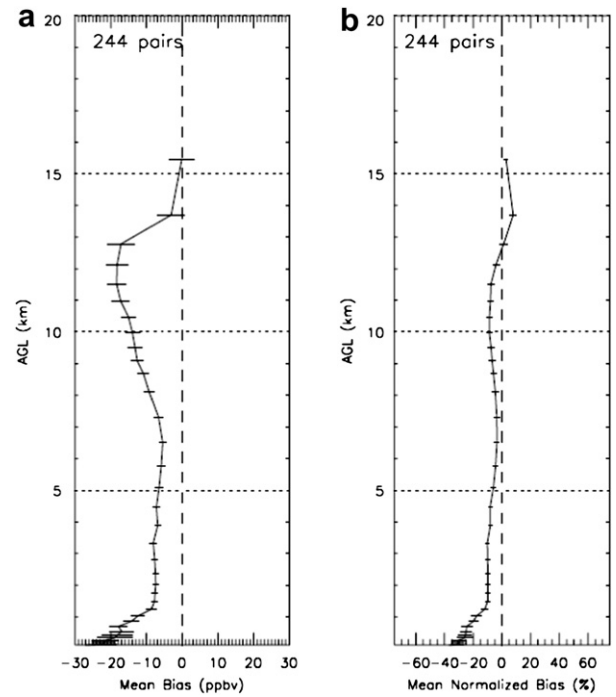


**Fig. 6.** OMI/ozonesonde comparison on 39 CMAQ vertical layers. Mean bias  $\left(\frac{1}{N} \sum_{i=1}^N (O_{3i}^{\text{OMI}} - O_{3i}^{\text{ozonesonde}})\right)$  and mean-normalized bias  $\left(\frac{1}{N} \sum_{i=1}^N \frac{(O_{3i}^{\text{OMI}} - O_{3i}^{\text{ozonesonde}})}{O_{3i}^{\text{ozonesonde}}}\right)$  from 244 pair of observations are presented, as well as the standard errors. For many of the observations, OMI did not extend below ~2-km, thus the statistics below about 2-km (model layers 1–17) are not reliable as they represent a small sample. For example, the number of pairs for model layers 5 through 11 is 1, 3, 3, 3, 7, 8, and 10, respectively.

mesoscale model (known as MM5) which provides pressure field for CMAQ. Extrapolation of OMI profile can usually make estimates at 1000 mb; however, considering the complication of ozone concentration at the surface layer, we decided to set missing values instead of using estimates from extrapolation.

### 3.2.3. Nearest-neighbor re-sampling Algorithm

OMI ozone re-sampled on CMAQ (both horizontally and vertically) may have missing values due to: (1) cloud contamination in the original OMI data; (2) mismatching pressures between OMI and CMAQ. To fill in a CMAQ grid where an OMI  $O_3$  observation is missing, we simply average the available OMI  $O_3$  values from its surrounding 8 CMAQ grids and assign this average value to it. Through this process, missing values in the middle-to-upper troposphere are mostly removed; however, in the boundary layer, numerous missing values still exist due to a mismatched pressure problem. Finally, we get a total of 244 OMI-ozonesonde pairs for the August 2006 period over the CMAQ model domain.

### 3.3. Comparison results

We calculate the mean bias  $\left(\frac{1}{N} \sum_{i=1}^N (O_{3i}^{\text{OMI}} - O_{3i}^{\text{ozonesonde}})\right)$  and mean normalized bias  $\left(\frac{1}{N} \sum_{i=1}^N \frac{(O_{3i}^{\text{OMI}} - O_{3i}^{\text{ozonesonde}})}{O_{3i}^{\text{ozonesonde}}}\right)$  as well as the standard errors, for the 267 pairs of OMI-sonde observations over OMI vertical resolution (Fig. 5) and the 244 pairs of OMI-sonde observations over CMAQ vertical resolution (Fig. 6). In both comparisons, OMI shows a reasonable agreement with ozonesonde

in the lower- to mid-troposphere. In the upper troposphere, while the bias increases, the normalized bias does not show much variation and remains below 10%. This small variation is due to the fact that the background ozone concentration in the upper troposphere is much higher than that in the lower- to mid-troposphere. In the upper troposphere, even a 20 ppb difference has a relatively small impact to the same variance applied to the lower- to mid-troposphere. In Fig. 6, the statistics between surface and ~2 km above the ground, which covers ~17 CMAQ layers, are not reliable as the sample sizes for these layers are particularly small due to missing OMI values in the boundary layer. These missing OMI values are mainly caused by the mismatch pressure problem discussed in section 3.2. The number of pairs drastically jumps from 87 in layer 15 (about 1.5 km) to 226 in layer 16 (about 1.8 km). As evident from Fig. 6, the bias decreases as the number of coincidence pairs (sample size) increases from the surface to ~2 km above the ground.

#### 4. Evaluation OMI O<sub>3</sub> with EPA surface-ozone monitoring data

In mid-latitude summer, the OMI retrievals have effective photon penetration depth in 800–900 hPa for tropical clear conditions (Liu et al., 2010). So for the first layer, the retrievals have 40–70% sensitivity and are captured in the total ozone. However, not all of them can be captured in the first layer due to inadequate vertical sensitivity.

OMI overpass time is about 1:30 PM local time. At this time, during August, the boundary layer is usually well mixed. We compare OMI measurements at the lowest layer (from surface to 2.5 km altitude) with daily ozone observations at 1400 local time from EPA's surface monitors for July 15 through September 7, 2006 (Fig. 7). OMI observations stay close to the mean-observed concentrations and do not exhibit much variation from the mean value, while surface monitors show a much larger variation, approximately double that of OMI's variation. The correlation

between the two observations is low (the correlation coefficient is 0.14). For OMI, the mean and standard deviation are 48.2 and 7.9, respectively, while for surface monitors, the mean and standard deviation are 48.9 and 16.7, respectively.

However, we should keep in mind that: (1) OMI observations are representing a volume-averaged quantity for a relatively large volume of air, while surface observations are point measurements. (2) Local emissions impact a substantial number of surface monitors; there is a large spatial variability even for stations only separated by a few kilometers. These observations somehow explain why OMI can observe neither the elevated surface concentrations nor the large variations experienced by the surface monitors.

Generally, the sensitivity of OMI to boundary layer ozone is limited. Furthermore, the retrieved ozone at 0–2.5 km layer maybe more sensitive to ozone at higher altitudes due to the coarse vertical resolution of OMI retrievals. That explains why the retrieved ozone from the first layer mainly reflects the climatological a priori values and underestimates the surface ozone variability. When there is stronger correlation between surface ozone and lower/middle tropospheric ozone, OMI retrievals maybe better used to represent surface ozone as a result of sensitivity to ozone at higher altitudes.

We compared the spatial distribution for OMI and surface monitors on August 3, 21, and 31, 2006 (Fig. 8). On August 3 and 21, there is a general agreement between OMI observations and the surface monitors. While OMI underestimates elevated ozone concentrations, it is able to explain the larger-scale spatial variation seen in the surface monitors. Under cloudy conditions, OMI overestimated ozone concentrations. But on August 31, OMI and surface monitors show substantial discrepancies in their respective datasets, and OMI completely misses the surface observations. Normally, OMI retrievals (either first layer or tropospheric ozone column) can better represent surface ozone under favorable meteorological condition (e.g., high pressure system), when there is stronger correlation between surface ozone and ozone at higher altitudes.

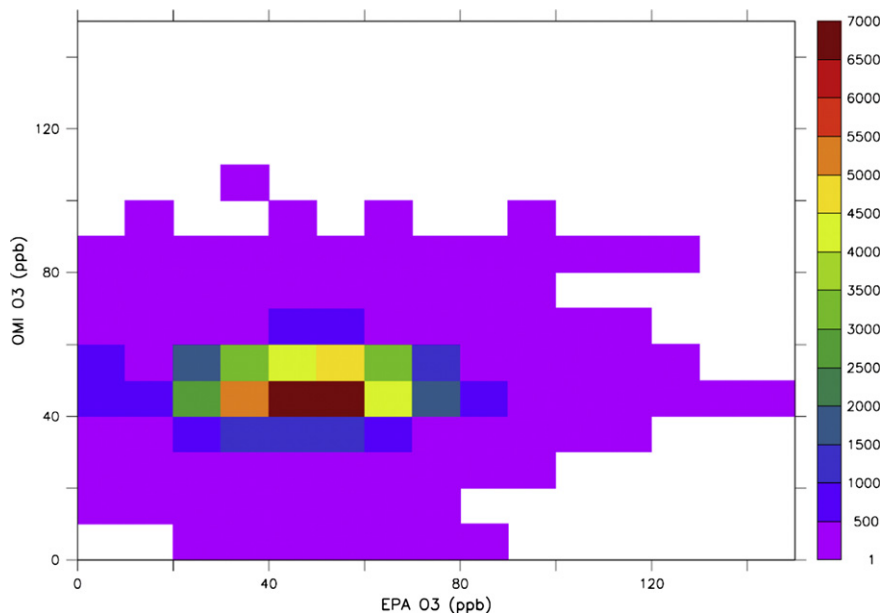


**Fig. 7.** 2D density plot showing numbers of coincidence pairs between OMI ozone observations in the boundary layer (surface to about 2.5 km altitude) and observations from EPA's surface monitors for July 15 through September 7, 2006. The pairs are constructed by extracting daily surface observations at 14:00 local time and pairing them with OMI observations. The figure indicates that OMI is not able to neither explain elevated surface concentrations nor the large variations experienced by the surface monitors. The correlation coefficient is 0.14, while the mean and standard deviation for OMI are 48.2 and 7.9, respectively and for surface monitors are 48.9 and 16.7, respectively.

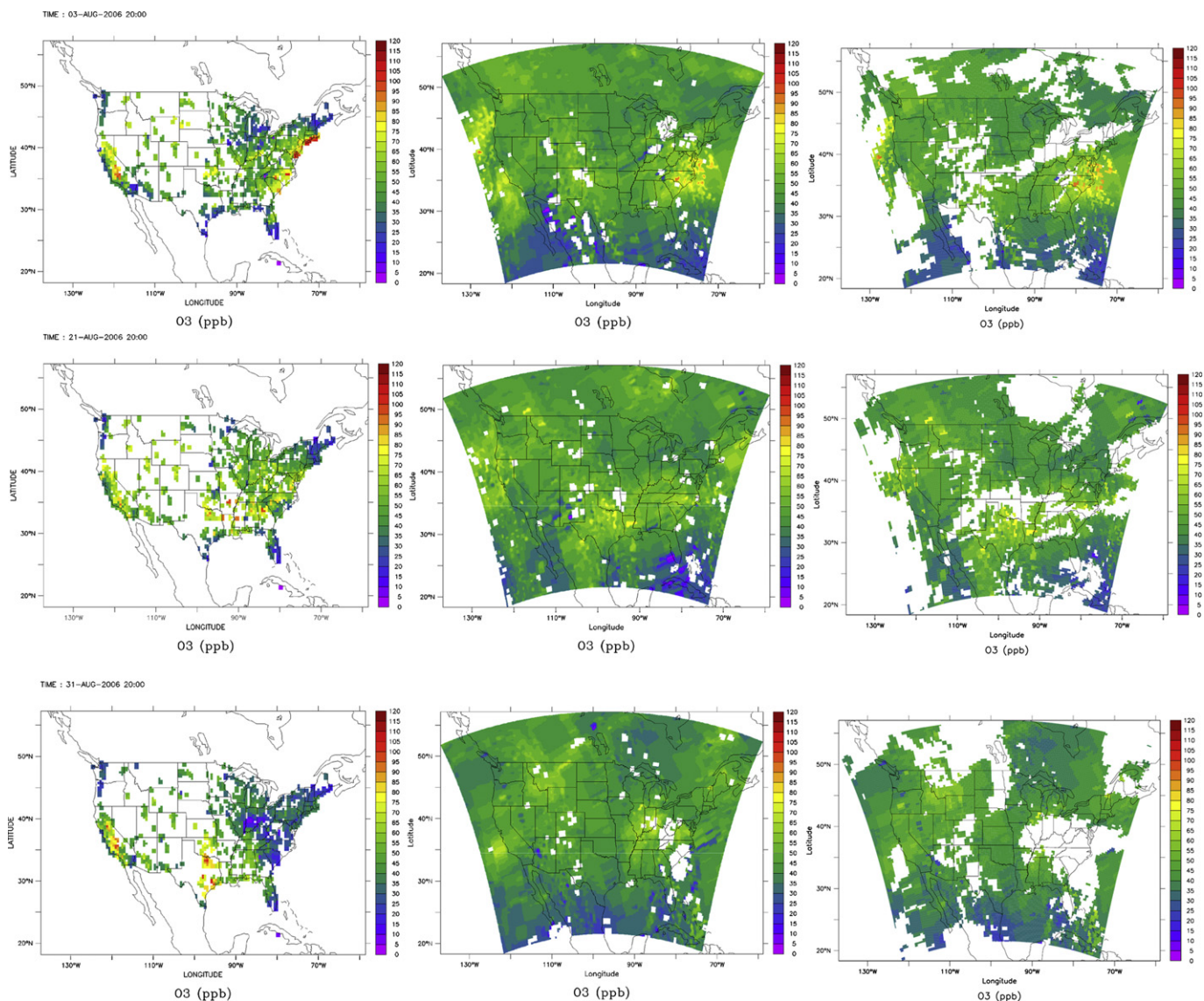


**Fig. 8.** EPA surface monitoring data (left panel) versus OMI ozone observations (middle panel: original OMI; right panel: OMI with cloud filter-data with cloud fraction  $>0.3$  are removed) for August 3, 21, and 31, 2006. Although August 3 and 21 show better agreements between the spatial patterns, OMI observations on August 31 are not representative of the boundary layer.

## 5. Conclusion

We evaluate the Ozone Monitoring Instrument (OMI) ozone-profile retrievals against ozonesonde data and EPA's surface measurements for August 2006. OMI ozone profile can explain the general vertical variation of ozone but is limited in observing the boundary layer ozone. Pair-wise comparisons between OMI and ozonesonde data for August 2006 show that OMI agrees reasonably with ozonesonde in the lower- to mid-troposphere. In the upper troposphere, while the bias increases, the normalized bias does not show much variation and remains below 10%. This is consistent with results of OMI validation against long-term ozonesonde data for 2004–2008 which states that OMI retrievals in the troposphere agree with ozonesonde observations to within 10% at middle latitudes (30N–60N). Comparison with EPA's surface-monitoring data indicates that OMI observations at the lowest layer (surface to 2.5 km altitude) represent the mean values. While OMI underestimates elevated ozone concentrations, it is able to explain the larger-scale spatial variation seen in the surface monitors.

OMI ozone profile data, re-sampled onto CMAQ modeling domain, has been used to specify lateral boundary conditions above 2 km altitude (considering OMI's boundary layer deficiency) for a simulation that spanned over August 2006. The model prediction of ozone is significantly improved and agrees better with the ozonesonde measurements. This improvement results from both representing the free-tropospheric ozone amounts more accurately and representing recirculating air masses more accurately. By modifying modeled  $O_3$  with OMI  $O_3$  throughout the model domain once a model-day, further improvement occurs, especially in the continental interior region where influences from the boundary conditions are small (Pour-Biazar et al., *in press*).

## References

- Levelt, P.F., Hilsenrath, E., Leppelmeier, G.W., van den Oord, G.H.J., Bhartia, P.K., Tamminen, J., de Haan, J.F., Veeckind, J.P., 2006. Science objectives of the Ozone Monitoring Instrument. *IEEE Trans. Geosci. Remote Sens.* 44 (5), 1199–1208.

- Liu, X., Bhartia, P.K., Chance, K., Spurr, R.J.D., Kurosu, T.P., 2010. Ozone profile retrievals from the ozone monitoring instrument. *Atmos. Chem. Phys.* 10, 2521–2537.
- Liu, X., Chance, K., Kurosu, T.P., 2007. Improved ozone profile retrievals from GOME data with degradation correction in reflectance. *Atmos. Chem. Phys.* 7, 1575–1583.
- Liu, X., Sioris, C.E., Chance, K.V., Kurosu, T.P., Newchurch, M.J., Martin, R.V., Palmer, P.L., 2005. Mapping tropospheric ozone profiles from an airborne ultraviolet-visible spectrometer. *Appl. Opt.* 44 (16), 3312–3319.
- Pour-Biazar, A., Khan, M., Wang, L., Park, Y.-H., Newchurch, M.J., McNider, R.T., Liu, X., Byun, D.W., Cameron, R., The utilization of satellite observation of ozone and aerosols in providing initial and boundary conditions for regional air-quality studies. *J. Geophys. Res.*, in press.
- Rodgers, C.D., 2000. *Inverse Methods For Atmospheric Sounding*. World Scientific Publishing Co. Pte. Ltd., New Jersey.
- Rodgers, C.D., Connor, B.J., 2003. Intercomparison of remote sounding instruments. *J. Geophys. Res.* 108 (D3), 4116.
- Thompson, A.M., Yorks, J.E., Miller, S.K., Witte, J.C., Dougherty, K.M., Morris, G.A., Baumgardner, D., Ladino, L., Rappenglueck, B., 2008. Tropospheric ozone sources and wave activity over Mexico City and Houston during MILAGRO/Intercontinental Transport Experiment (INTEX-B) Ozonesonde Network Study, 2006 (IONS-06). *Atmos. Chem. Phys.* 8, 5113–5125.
- Worden, J., Liu, X., Bowman, K., Chance, K., Beer, R., Eldering, A., Gunson, M., Worden, H., 2007. Improved tropospheric ozone profile retrievals using OMI and TES radiances. *Geophys. Res. Lett.* 34, L01809.
- Ziemke, J.R., Chandra, S., Bhartia, P.K., 2001. “Cloud slicing”: a new technique to derive upper tropospheric ozone from satellite measurements. *J. Geophys. Res.* 106, 9853–9867.